Confined quantum systems: The parabolically confined hydrogen atom

1998 J. Phys. A: Math. Gen. 31 4493

(http://iopscience.iop.org/0305-4470/31/19/014)

J. Phys. A: Math. Gen. **31** (1998) 4493–4520. Printed in the UK PII: S0305-4470(98)86913-8

Confined quantum systems: The parabolically confined hydrogen atom

D S Krähmer†, W P Schleich† and V P Yakovlev‡

† Abteilung für Quantenphysik, Universität Ulm, 89069 Ulm, Germany

‡ Moscow State Engineering Physics Institute, 115409 Moscow, Russia

Received 18 August 1997, in final form 9 February 1998

Abstract. We investigate a hydrogen-like atom (or any other system with a Coulomb potential) confined to a space which is bounded by a paraboloid. The nucleus of the atom resides at the focus of the paraboloid and we require the electronic wavefunction to vanish on the paraboloid. We derive an exact implicit analytic solution to the problem and also explicit analytic expressions for the wavefunctions and eigenenergies in the so-called strong-shift regime. We also discuss the influence of the boundary on the permanent dipole moments of the eigenstates. Finally, we investigate this system in WKB-approximation and give the Bohr–Sommerfeld quantization rule which is different from the usual rule due to the new boundary condition.

1. Introduction

In this paper we deal with a kind of problem which is almost as old as quantum mechanics itself. Usually one considers quantum systems in an infinite environment, i.e. the boundary conditions are at infinity. Many of the standard problems in quantum mechanics such as the harmonic oscillator or the hydrogen atom are solved with vanishing wavefunctions at infinity. The energy spectra as we know them are calculated for this specific choice of boundary conditions. Of course, in many situations it is well justified to use these boundary conditions and usually they simplify the mathematics of the problem. However, there are also situations in which the model of a confined quantum system can be used as a good approximation. A prominent field where confined quantum systems are important is semiconductor physics and in particular quantum wells, wires, and dots. In section 2 we will give an overview of the history of confined quantum systems from its discovery in 1937 until recent years.

It is not our intention here to develop a theory for a specific experimental situation, we rather want to demonstrate for a simple model system the effects which may occur. We concentrate on a hydrogenic system, i.e. a particle moving in a Coulomb potential. As a non-standard boundary in our problem we consider a paraboloid with the Coulomb centre located at the focus. The motivation for taking a paraboloid is more of a mathematical origin than of a physical one: This type of boundary can easily be described in parabolic coordinates, and using them to solve the three-dimensional Schrödinger equation allows for a separation into three ordinary differential equations. The possibility for a separation of variables is the basis for many theoretical investigations. In the context of confined quantum systems the starting point for analytical calculations is to find all coordinate systems in which the Schrödinger equation of the system separates. Then the surfaces of a constant coordinate

0305-4470/98/194493+28$19.50

are the natural boundaries for which confinement of the system can be taken into account in the easiest way.

Our choice of the boundary in the form of a paraboloid is based on the separability of the Schrödinger equation in parabolic coordinates. The fact that the standard solutions with boundary conditions at infinity have a quite simple analytical form makes this problem even more attractive at least from a mathematical point of view.

Little work has been done for this case. You *et al* [1] were the first to use this as a model for a substitutional and/or interstitial surface atom. They were only interested in the ground state. More extensive work has been done by Ley-Koo and García-Castelán [2]. They also considered the energy shift of some excited states, and for the ground state they calculated the hyperfine splitting and the electric dipole moment. It is the purpose of this paper to give a more complete picture of the energy spectrum, not only for the first few excited states. We will discuss the properties of the whole (discrete) spectrum and in particular we will consider the most interesting case, namely when there is a large shift of the energy levels.

In section 3 we investigate by using analytical methods the properties of a hydrogen atom confined in a paraboloidal geometry. We discuss in detail peculiarities in the spectrum and show some typical examples for the wavefunctions.

In order to gain more insight into the underlying physics we devote section 4 to a semiclassical analysis of this problem. We will show that the usual Bohr–Sommerfeld quantization rule has to be modified in the presence of the boundary. When this is taken into account one finds a very good agreement with the exact solution given in section 3. Whereas in the free problem the parabolic quantum numbers run from zero to infinity, this is no longer true for the confined system. Using the semiclassical approach one can get a more intuitive understanding of why and how these quantum numbers are limited. Of course, purely numerical methods are an appropriate means for obtaining solutions in many practical cases. However, the semiclassical approach also offers advantages, mainly in two respects. (i) As already pointed out, it gives a deeper insight into the physics of the problem (at the cost of accuracy of the solution). (ii) It is very well suited for the determination of approximate eigensolutions which in turn can be used as a starting point for an efficient purely numerical solution.

2. A brief history of confined quantum systems

In most of the familiar stationary problems of quantum mechanics one does not restrict the size of the system. Then the eigenfunctions are calculated uniquely by requiring that they should vanish at infinity. In certain physical situations, however, it is useful to consider a model where a system is confined by infinitely high potential walls. Then the wavefunction of the system has to vanish on a certain boundary which lies at finite distances but may extend until infinity. It is the aim of this section to give an overview of the history of such confined quantum systems. We will list all the systems which (to our knowledge) have been investigated, and discuss practical applications. A more detailed discussion of this history can be found in [3].

2.1. Confined atoms and molecules

Historically, a confined hydrogen atom was considered for the first time by Michels *et al* [4]. Similar investigations have been performed for hydrogen [5, 6] and helium [7, 8] in spherical boxes. The WKB-approximation in this context was used for the first time

by Dingle [9]. Based on an experiment concerned with hydrogen atoms enclosed in α-quartz [10] several models in the form of confined quantum systems have been investigated [11–16]. The case of a hydrogen atom in a soft spherical box was investigated in [23].

When Wigner investigated some aspects of perturbation theory [17] he initiated a series of papers [18–21] which indirectly contributed to the problem of confined quantum systems.

It is well known that the Schrödinger equation for the hydrogen atom is also separable in parabolic coordinates. The problem of a hydrogen atom in a symmetrical box with paraboloidal boundaries was treated in [24]. A simplification consists of dropping one of the paraboloids. This is exactly the model we will treat in sections 3 and 4.

A further coordinate system which allows for the separation of the Schrödinger equation is the prolate spheroidal coordinate system. The problem of a hydrogen molecule ion in a spheroidal box was treated by several authors [25, 26, 15, 27]. The hydrogen molecule in the same environment was treated in [28, 29] and the hydrogen atom in [24].

Of great importance in surface physics are systems which are bounded by a plane, or have a plane interface. The mathematically simplest problem of this type is a hydrogenic system with its centre located *on* the plane surface and has been studied in [30, 31]. The prolate spheroidal coordinate system also allows for a separation in the case when the hydrogen atom is located at some distance away from the plane boundary. Investigations of this type of problem were published in [32–39]. The properties of a hydrogen molecule near a hard wall were investigated in [40].

2.2. The confined harmonic oscillator

Heretofore we have reported only on systems with Coulomb potentials. The harmonic oscillator represents another system of central importance to quantum mechanics, and its properties were also investigated when it is enclosed in hard boxes. In connection with an astrophysical problem, Chandrasekhar [41] was one of the first to briefly touch upon the problem of a bounded linear harmonic oscillator. Further work on this problem has been published in [42–44, 46, 47, 49, 50]. The inverted harmonic oscillator was treated in [48] and the three-dimensional harmonic oscillator was investigated in [22, 51].

A WKB-treatment of the problem was presented by Vawter [45] together with an exact solution in the form of series expansions. He found that in general the results of the two methods are in good agreement but in the case when a classical turning point comes close to the boundary the semiclassical method becomes inaccurate. We will return to this issue in section 4 where we discuss the reason for this deviation and give a solution to the problem.

2.3. Other systems and general theories

The most simple confined quantum system is, of course, a free particle in a box. Of all confined quantum systems one can think of, this is certainly the most simple one and the solution of the corresponding Schrödinger equation can be found in any introductory textbook on quantum mechanics. Fowler [22] calculated the polarizability for an electron in a one-dimensional box and also for three-dimensional spherical and cubic boxes.

The restricted rotor was investigated by Sommerfeld and Hartmann [52] and the anharmonic oscillator with a x^{2m}-potential (m integer) was treated by Chaudhuri and Mukherjee [53] who calculated the even- and odd-parity eigenvalues as the roots of explicitly derived functions.

Apart from solving specific examples there have also been some efforts in developing more general theories. The earliest paper in this direction was published by Froehlich [54]

who invented a kind of boundary perturbation theory. A more recent similar approach is due to Berman [55]. Wassermann [56] developed a very general theory which is not limited to the Schrödinger equation. Naturally, it is very technical and of limited practical use. Gonda and Gray [57] wrote a paper on boundary perturbation theory along the lines of ordinary perturbation theory.

Hull and Julius [58] gave a formula for the shift of an energy level of a one-dimensional system which is valid in the 'neighbourhood' of any known solution. This formula was applied by Singh [26] to the H_2^+ ion. The method was modified by Gorecki and Byers Brown [59] to work as an iterative procedure. Two years later they presented a combination of boundary perturbation theory with a variational technique [60] which can even be applied to non-separable cases. In their paper they treated for the first time the problem of a hydrogen atom in a spherical box where the nucleus is fixed off-centre. Variational methods have been discussed in [61–66].

A completely different approach is based on hypervirial theorems [67]. They may be used in order to obtain a perturbation expansion for the energy in which each order is expressed solely in terms of the unperturbed energy [68]. Fernández and Castro [69] used such hypervirial relations to investigate enclosed quantum systems. In the following two years they published a whole series of papers in which they applied this method to all kinds of systems. In the paper by Arteca *et al* [70] a summary of the method and a comprehensive list of references can be found.

Finally we want to mention the so-called embedding method developed by Inglesfield [71] and applied to confined quantum systems by Crampin *et al* [72].

2.4. Applications

The model of a one-electron atom confined in a hard spherical box has been used in the context of partially ionized plasmas [73] and for studying thermodynamic properties of non-ideal gases [74].

Brady and Rowell [75] reported that there is some evidence for the emission of electrons in rocks under compression up to the point of fracture. It was suggested that a confined atom could serve as a model for the phenomenon.

Kanorsky *et al* [76, 77] investigated the properties of foreign atoms implanted in solid and liquid helium. They observed pressure broadening and a shift of the excitation and emission lines. They explained the observed spectra by assuming a bubble structure of the trapping sites for the atoms. A summary can be found in their Les Houches lecture [78].

Electron–electron and electron–hole interactions in small semiconductor crystallites have been investigated theoretically by, e.g. Brus [79] and Schmidt and Weller [80].

Since the 1980s the most important applications of confined quantum systems are quantum wells, quantum well wires and quantum dots. The properties of a hydrogenic impurity in a quantum well was investigated by Bastard [81]. Bryant [82] investigated the spectrum of an on-axis Coulomb centre in a cylindrical box. Brown and Spector [83] were the first to generalize this to an off-centre Coulomb potential using a variational method. The technique of Diamond *et al* [65] was applied to the same system by Tsonchev and Goodfriend [84]. Recently, Zhu and Chen [85] examined the problem of an off-centre Coulomb potential inside a spherical box with a finite potential wall as a model for a quantum dot.

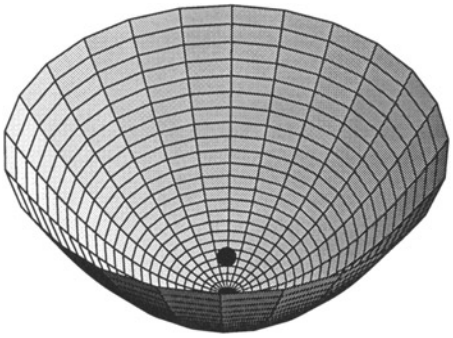

Figure 1. Schematic illustration of the model. The nucleus of a single-electron atom resides at the focus of a paraboloid. The assumption is that the electron cannot penetrate through this boundary and hence the wavefunction of the electron must vanish on the surface of the paraboloid.

3. The hydrogen atom with a paraboloidal boundary

When solving partial differential equations analytically the most important issue is the separability of the equation in order to obtain a set of ordinary differential equations which can be treated much easier. In the case of the hydrogen atom there are four coordinate systems in which the Schrödinger equation separates. These are the spherical, parabolic, prolate spheroidal, and the sphero-conical coordinates (for a review see, e.g. [86, 87]).

In this section we consider a hydrogen atom confined to a region of space which is bounded by a paraboloid of revolution. The nucleus of the atom is fixed at the focus of the paraboloid as shown schematically in figure 1. We are interested in all the (bound) states of this system, their energies and the spatial structure of their wavefunctions.

We first review the parabolic eigenstates of the hydrogen atom in free space and then derive an implicit analytical solution for the problem with a paraboloidal boundary. As we will see in this section, there are situations where the energy levels of the confined hydrogen atom are strongly shifted compared with a free atom. For this 'strong-shift regime' we derive explicit analytical expressions for the eigenstates and eigenenergies. Finally, we investigate the influence of the boundary on the permanent dipole moments of the eigenstates.

3.1. Review of parabolic eigenstates

Parabolic coordinates are defined by

$$x = \sqrt{\xi\eta}\cos\varphi \qquad y = \sqrt{\xi\eta}\sin\varphi \qquad z = \tfrac{1}{2}(\xi - \eta)$$

where $0 \leqslant \xi,\ \eta < \infty$ and $0 \leqslant \varphi < 2\pi$. Figure 2 helps to visually understand the meaning of the coordinates ξ and η. The Laplacian reads

$$\Delta = \frac{4}{\xi + \eta}(\partial_\xi \xi \partial_\xi + \partial_\eta \eta \partial_\eta) + \frac{1}{\xi\eta}\partial_\varphi^2$$

where $\partial_\xi = \partial/\partial\xi$, $\partial_\eta = \partial/\partial\eta$ and $\partial_\varphi = \partial/\partial\varphi$. The Schrödinger equation

$$\left(-\frac{\hbar^2}{2m}\Delta - \frac{Ze^2}{r}\right)\psi = E\psi$$

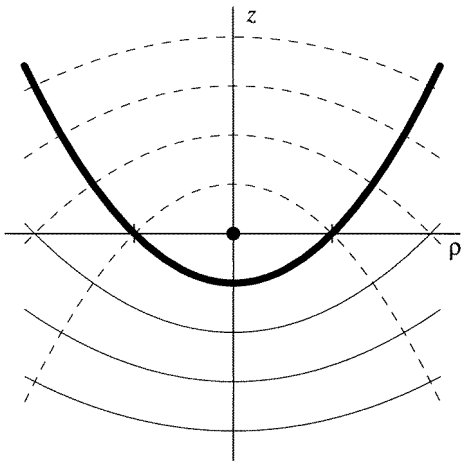

Figure 2. Illustration of parabolic coordinates. We show cuts through surfaces of constant ξ (broken curves) and constant η (full curves). The heavy full curve indicates the position of the boundary. The coordinate $\rho = \sqrt{x^2 + y^2}$.

for a single-electron atom with nuclear charge $Z|e|$ reads, in parabolic coordinates,

$$\frac{4}{\xi' + \eta'}(\partial_{\xi'}\xi'\partial_{\xi'} + \partial_{\eta'}\eta'\partial_{\eta'})\psi + \frac{1}{\xi'\eta'}\partial_{\varphi}^2\psi + \left(2E' + \frac{4}{\xi' + \eta'}\right)\psi = 0 \qquad (1)$$

where we have introduced dimensionless coordinates ξ', η' and energy E' via

$$\xi = a_0\xi \qquad \eta = a_0\eta' \qquad E = \frac{Ze^2}{a_0}E'$$

with

$$a_0 = \frac{\hbar^2}{Zme^2}$$

being the Bohr radius. In the remainder of this paper we will always use these dimensionless units and therefore drop the primes for simplicity.

We start with an ansatz of the form

$$\psi(\xi, \eta, \varphi) = f_1(\xi)f_2(\eta)\mathrm{e}^{\mathrm{i}m\varphi}$$

where m is an integer. Substituting this ansatz into the Schrödinger equation (1) we find the equations for the functions f_1 and f_2:

$$\partial_\xi\xi\partial_\xi f_1 + \left(\frac{1}{2}E\xi - \frac{m^2}{4\xi} + Z_1\right)f_1 = 0 \qquad (2a)$$

and

$$\partial_\eta\eta\partial_\eta f_2 + \left(\frac{1}{2}E\eta - \frac{m^2}{4\eta} + Z_2\right)f_2 = 0 \qquad (2b)$$

where Z_1 and Z_2 are constants of separation satisfying the condition $Z_1 + Z_2 = 1$. Since here we are interested only in bound states with negative energy†, we introduce a new

† It would also be interesting to consider scattering states with positive energy. Because of the specific properties of a paraboloid, a plane wave travelling along the symmetry axis (without Coulomb potential) would be focused at the origin and leave the paraboloid in the opposite direction. When we now consider the scattering of an electron

variable for the energy

$$E = -\frac{1}{2n^2} \qquad \text{or} \qquad n = \frac{1}{\sqrt{-2E}}.$$

The general solutions of equations (2*a*) and (2*b*) which are regular at the origin are

$$f_1(\xi) = \xi^{\frac{1}{2}|m|} \exp\left(-\frac{\xi}{2n}\right) \Phi(\tfrac{1}{2}|m| + \tfrac{1}{2} - nZ_1, |m| + 1, \xi/n) \tag{3a}$$

and

$$f_2(\eta) = \eta^{\frac{1}{2}|m|} \exp\left(-\frac{\eta}{2n}\right) \Phi(\tfrac{1}{2}|m| + \tfrac{1}{2} - nZ_2, |m| + 1, \eta/n) \tag{3b}$$

where $\Phi(\alpha, \gamma, z)$ denotes the confluent hypergeometric function. When we impose the standard boundary conditions,

$$f_{1,2} \to 0 \qquad \text{for } \xi, \eta \to \infty$$

we find that the first parameters of the confluent hypergeometric functions must be non-negative integers, i.e.

$$\tfrac{1}{2}|m| + \tfrac{1}{2} - nZ_1 = -n_1 \tag{4a}$$

and

$$\tfrac{1}{2}|m| + \tfrac{1}{2} - nZ_2 = -n_2 \tag{4b}$$

and also that Φ simplifies to a Laguerre polynomial

$$L_{n_1}^{|m|}(z) = \binom{n_1 + |m|}{n_1} \Phi(-n_1, |m| + 1, z).$$

Summing equations (4*a*) and (4*b*) and using the condition $Z_1 + Z_2 = 1$ yields

$$n = n_1 + n_2 + |m| + 1 \tag{5}$$

which means that in free space n must be an integer.

This completes the result for the parabolic eigenstates and their spectrum. To summarize, the eigenstates read

$$\psi_{n_1,n_2,m}(\xi, \eta, \varphi) = \mathcal{N}(\xi\eta)^{\frac{1}{2}|m|} \exp\left(-\frac{\xi + \eta}{2n}\right) L_{n_1}^{|m|}(\xi/n) L_{n_2}^{|m|}(\eta/n) \mathrm{e}^{\mathrm{i}m\varphi}$$

where

$$\mathcal{N} = \frac{1}{\sqrt{\pi} n^{|m|+2}} \sqrt{\frac{n_1! n_2!}{(n_1 + |m|)!(n_2 + |m|)!}}$$

is the normalization constant, and the corresponding energy eigenvalues are

$$E_n = -\frac{1}{2n^2} = -\frac{1}{2(n_1 + n_2 + |m| + 1)^2}.$$

and take into account the Coulomb centre, it is clear that it will be scattered from the paraboloid in the direction of the Coulomb centre independent of its impact parameter. Therefore, even for extremely large impact parameters the electron will finally interact strongly with the Coulomb potential in extreme contrast to usual scattering situations. It seems very interesting to investigate the wave mechanical equivalent, however, it is not clear how to formulate the asymptotic wavefunction which is the key point in scattering theory.

3.2. The solution with a paraboloidal boundary

We now change the boundary conditions to

$$f_1(\xi = \infty) = 0$$

and

$$f_2(\eta = \eta_0) = 0.$$

Solutions (3*a*) and (3*b*) are still valid. However, with the new boundary conditions the energy parameter n will no longer be an integer. We therefore replace the symbol n by ϵ. Since we did not change the boundary condition for the ξ-coordinate, the solution f_1 still simplifies to a Laguerre polynomial. The only difference is that n has to be replaced by ϵ, i.e.

$$f_1(\xi) = (-1)^{n_1} n_1! \xi^{\frac{1}{2}|m|} \exp\left(-\frac{\xi}{2\epsilon}\right) L_{n_1}^{|m|}(\xi/\epsilon). \tag{6}$$

However, the function f_2 is no longer a simple polynomial. The only thing necessary is to eliminate Z_2 from the first parameter of Φ in equation (3*b*). By using $Z_1 + Z_2 = 1$ and equation (4*a*) with n replaced by ϵ, we find for this first parameter

$$\tfrac{1}{2}|m| + \tfrac{1}{2} - \epsilon Z_2 = n_1 + |m| + 1 - \epsilon. \tag{7}$$

Hence, we can write

$$f_2(\eta) = \eta^{\frac{1}{2}|m|} \exp\left(-\frac{\eta}{2\epsilon}\right) \Phi(n_1 + |m| + 1 - \epsilon, |m| + 1, \eta/\epsilon)$$

and the equation

$$\Phi(n_1 + |m| + 1 - \epsilon, |m| + 1, \eta_0/\epsilon) = 0 \tag{8}$$

determines the eigenvalues implicitly.

3.3. The strong-shift regime

It is a numerical task to extract the eigenvalues ϵ from equation (8). However, in a certain regime we can solve this equation approximately. For this purpose we use an expansion [88] of the confluent hypergeometric function Φ in terms of Bessel functions

$$\Phi(\alpha, \gamma, z) = \Gamma(\gamma) \mathrm{e}^{z/2} \left(\frac{1}{2}\gamma z - \alpha z\right)^{(1-\gamma)/2} \sum_{l=0}^{\infty} A_l \left(\frac{z}{2\gamma - 4\alpha}\right)^{l/2} J_{\gamma-1+l}\left(\sqrt{2\gamma z - 4\alpha z}\right)$$

where the coefficients A_l are defined by

$$A_0 = 1 \qquad A_1 = 0 \qquad A_2 = \tfrac{1}{2}\gamma$$
$$(l+1)A_{l+1} = (l + \gamma - 1)A_{l-1} + (2\alpha - \gamma)A_{l-2}.$$

If the condition

$$\left|\frac{z}{2\gamma - 4\alpha}\right| \ll 1 \tag{9}$$

is fulfilled then we only have to keep the first term of the expansion and we can approximate the confluent hypergeometric function by

$$\Phi(\alpha, \gamma, z) \approx \Gamma(\gamma) \mathrm{e}^{z/2} (\tfrac{1}{2}\gamma z - \alpha z)^{(1-\gamma)/2} J_{\gamma-1}\left(\sqrt{2\gamma z - 4\alpha z}\right).$$

In our case the parameters of Φ are

$$\alpha = n_1 + |m| + 1 - \epsilon$$
$$\gamma = |m| + 1$$
$$z = \eta_0/\epsilon$$

and condition (9) reads

$$\frac{\eta_0}{4\epsilon(\epsilon - \tilde{n}_1)} \ll 1 \tag{10}$$

where we have introduced

$$\tilde{n}_1 = n_1 + \tfrac{1}{2}(|m| + 1).$$

We call inequality (10) the strong-shift condition. It is fulfilled if either η_0 is small enough or the energy parameter ϵ is large enough. Then we find for f_2 the rather simple expression

$$f_2(\eta) = J_{|m|}\left(2\sqrt{\eta}\sqrt{1 - \tilde{n}_1/\epsilon}\right). \tag{11}$$

For the determination of the eigenenergies in this approximation we need the zeros of the Bessel functions. We denote the $(n_2 - 1)$th zero of $J_{|m|}$ by $j_{|m|,n_2}$ (> 0):

$$J_{|m|}(j_{|m|,n_2}) = 0 \qquad n_2 = 0, 1, 2, \ldots.$$

From the quantization condition

$$J_{|m|}\left(2\sqrt{\eta}_0\sqrt{1 - \tilde{n}_1/\epsilon}\right) = 0$$

we find the eigenvalues

$$\epsilon = \frac{\tilde{n}_1}{1 - j^2_{|m|,n_2}/(4\eta_0)}. \tag{12}$$

Since we must always have $\epsilon > 0$, we immediately see that there exist maximum values for the quantum numbers n_2 and $|m|$. The semiclassical treatment which is the topic of section 4 will give a more physical understanding of this fact.

We define $(n_2)_{\max}$ as the largest integer for a given m satisfying the inequality

$$j_{|m|,n_2} \leqslant 2\sqrt{\eta_0}.$$

$|m|_{\max}$ is defined as the largest integer satisfying the inequality

$$j_{|m|,0} \leqslant 2\sqrt{\eta_0}.$$

If we choose η_0 small enough so that $j_{0,0} > 2\sqrt{\eta_0}$ or $\eta_0 < \eta_c = j^2_{0,0}/4 \approx 1.45$ (Bohr radii), then there exist no bound states at all. We will discuss this in more detail in section 4.

Using the eigenvalues (12) and the wavefunction (11), we find for the complete eigenfunction

$$\tilde{\psi}_{n_1,n_2,m}(\xi, \eta, \varphi) = \tilde{\mathcal{N}}\xi^{\frac{1}{2}|m|}\exp\left(-\frac{\xi}{2\epsilon}\right)L^{|m|}_{n_1}(\xi/\epsilon)J_{|m|}\left(\sqrt{\eta/\eta_0}\,j_{|m|,n_2}\right)\mathrm{e}^{\mathrm{i}m\varphi}. \tag{13}$$

In the appendix we calculate the normalization constant $\tilde{\mathcal{N}}$ exactly with the result

$$\tilde{\mathcal{N}} = \frac{1}{\eta_0 J_{|m|+1}(j_{|m|,n_2})\sqrt{\pi n^{|m|+1}}}\sqrt{\frac{n_1!}{(n_1 + |m|)!}}\left(\frac{\epsilon}{\eta_0}\tilde{n}_1 + \frac{1}{6} + \frac{|m|^2 - 1}{3j_{|m|,n_2}}\right)^{-1/2}. \tag{14}$$

3.4. Discussion

In the preceding section we have calculated the spectrum and wavefunctions for the Coulomb problem with the new boundary condition. In this section we discuss these results, in particular, we will show how levels are shifted, how previously degenerate levels split, and how the wavefunctions are deformed by the boundary.

The spectrum of a hydrogen atom in free space is highly degenerate. The level with principal quantum number n has a degeneracy n^2. The reason for this degeneracy is the conserved spherical angular momentum symmetry and the conserved Runge–Lenz vector. By imposing the paraboloidal boundary these symmetries are broken and, therefore, the degeneracy is, at least partially, removed. Indeed, we have seen from our calculations that the eigenenergies depend on n_1, n_2 and $|m|$ (but not on the sign of m). Therefore, the levels with $m = 0$ are non-degenerate whereas all other levels are twofold degenerate.

Let us now discuss what happens to a single (n^2-fold degenerate) level n of a hydrogen atom when we put the boundary at $\eta = \eta_0$. If this boundary is very far away, so that classically the electron cannot reach it, then practically speaking the level remains degenerate as it was before. However, in a situation where the boundary is close to the nucleus, the splitting becomes larger and at a certain smaller value of η_0 it becomes important. For even smaller η_0 the original level with quantum number n will be split up in $\frac{1}{2}(n^2 + n)$ levels with increased energy. This number is the sum

$$\sum_{m=0}^{n-1} \sum_{n_1=0}^{n-m-1} 1$$

which counts the number of levels with different quantum numbers n_1, n_2, and $|m|$ (regardless of the sign of m) all belonging to the manifold labelled with n.

As we have seen in the preceding sections there are maximum allowed values for n_2 and $|m|$ which depend on η_0. If we continue to decrease η_0 and monitor the corresponding spectrum we will see that one level after the other will vanish which means that they are no longer bound states. This can clearly be seen in figure 3.

Heretofore we have looked at what happens to a *single* degenerate level of the unperturbed spectrum (without the boundary) characterized by the quantum number n. A slightly different way of looking at the spectrum is to consider several unperturbed levels simultaneously. In figure 4 we represent the spectrum by plotting the unperturbed levels $n = 1, \ldots, 6$ and their splitting as a function of η_0. However, for the sake of clarity we do not show *all* splitted levels but only a few of them.

We start by considering a small value of η_0, i.e. $\eta_0 < \eta_c$. In this case there are no bound states at all. This means that there are no levels with negative energy, but there are discrete levels in the effective potential for motion in the η-direction. The corresponding wavefunction has the character of a bound state only in the η-coordinate whereas it has the character of a scattering state in the ξ-coordinate. Pictorially, this means that the electron is confined to regions in space which have the shape of paraboloids. The electron is localized in the η-coordinate but is delocalized in the ξ-coordinate.

When we increase η_0, then at $\eta_0 = \eta_c$ something happens: in the effective potential for the motion in the η-direction the lowest level has zero energy. For a slightly larger value of η_0 the lowest level in the effective potential moves to a negative energy. In this case the only allowed value for n_2 is zero, that is, $(n_2)_{\max} = 0$. However, in the ξ-direction we have all values of $n_1 = 0, 1, \ldots$. This means that at $\eta_0 = \eta_c$ a whole set consisting of infinitely many levels (bound states) appears, with quantum numbers $n_2 = 0$, $n_1 = 0, 1, 2, \ldots$ and $m = 0$. At another, larger value of η_0 the second level in the effective potential crosses the

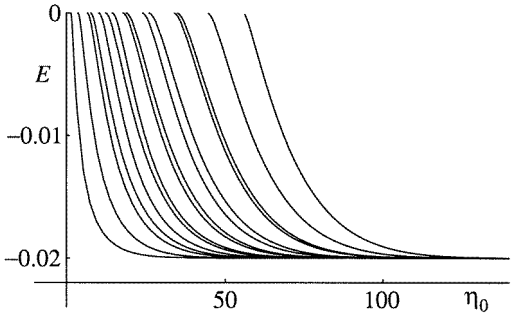

Figure 3. Splitting of the single, degenerate level $n = 5$ of free hydrogen. With decreasing η_0 the single level splits into 15 levels with an increased energy. Each of these levels vanishes at certain values of η_0, meaning that the corresponding state is no longer a bound state.

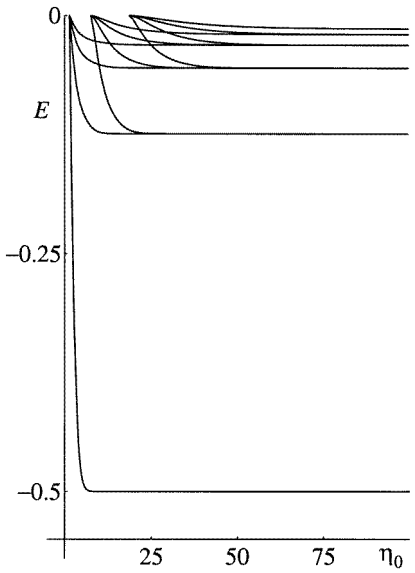

Figure 4. Part of the spectrum of a confined hydrogen atom as a function of η_0. For very small values of η_0 there are no bound states and therefore no levels. Then, for increasing η_0, levels corresponding to bound states appear. At certain discrete values of η_0 whole sets of infinitely many levels are born and gradually go down to their unperturbed values. Of course, only a few of them are shown in the figure.

zero-energy line and another set with infinitely many levels appears in the spectrum. They have the quantum numbers $n_2 = 1$, $n_1 = 0, 1, \ldots$. The same thing happens every time a level crosses the zero-energy line in the effective potential. In figure 4 we plot the spectrum as a function of the parameter η_0. At discrete values of η_0 one can see the birth of level sets. For clarity we have drawn only a few levels.

Finally, we discuss the spatial wavefunction of some eigenstates. There are two classes of states distinguished by the effect of the boundary on them. The parabolic eigenstates of a free hydrogen atom are well known, and they are the appropriate set of states to be used as a starting point for our problem. The two parabolic quantum numbers n_1 and n_2 are associated with the coordinates ξ and η. Let us first consider the case $n_1 > n_2$. This means that in the ξ-direction there is a higher excitation than in the η-direction. When we recall the geometrical meaning of ξ and η from figure 2 we see that in this case the electron cloud is concentrated in the region with positive z-values, as can be seen in figure 5(a). Analogously, for $n_1 < n_2$ it is concentrated in the region with negative z-values, shown in figure 5(c). In free space the state with parabolic quantum numbers n_1, n_2 and the state with n_1 and n_2 exchanged are perfectly symmetric with respect to the plane $z = 0$. However, if we include the boundary then we break the symmetry. In this case the states with $n_1 > n_2$ fit better into the space left by the boundary because the shape of the wavefunction is similar to that of the boundary. On the contrary, in the case $n_1 < n_2$ the wavefunction does not fit at all into the space left by the boundary. This causes a dramatic change in the electron distribution and also a large shift of the energy of the corresponding level.

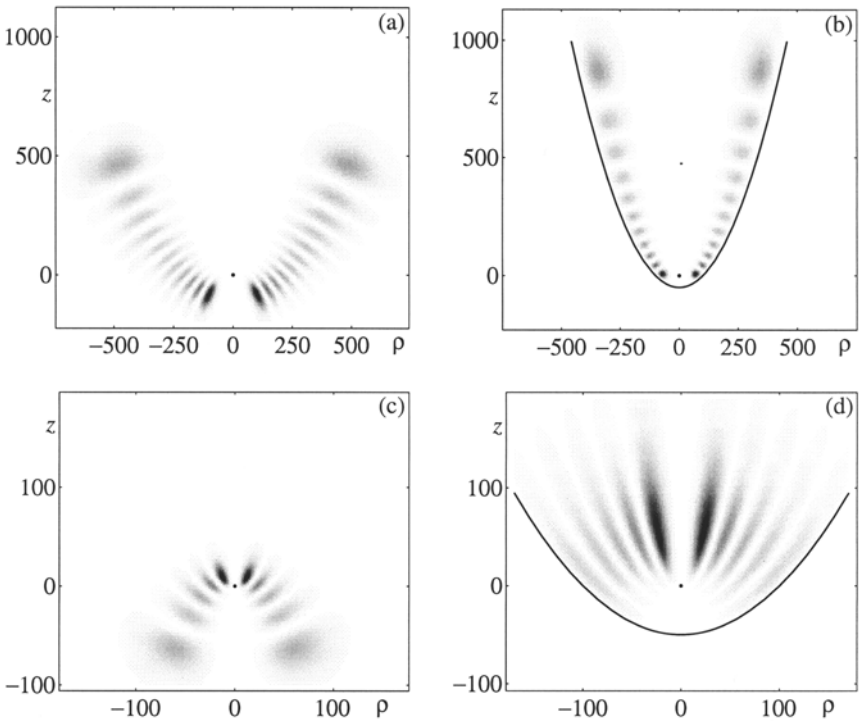

Figure 5. Typical wavefunctions of atomic hydrogen with and without a paraboloidal boundary. (*a*) $n_1 = 10$, $n_2 = 0$, $m = 10$ without a boundary. (*b*) $n_1 = 10$, $n_2 = 0$, $m = 10$ with a boundary. (*c*) $n_1 = 0$, $n_2 = 4$, $m = 3$ without a boundary. (*d*) $n_1 = 0$, $n_2 = 4$, $m = 3$ with a boundary. The coordinate $\rho = \sqrt{x^2 + y^2}$.

In the first case, where $n_1 > n_2$, the electron distribution is more localized as can be seen from figure 5(*b*). In the other case, where $n_1 < n_2$, there is a strong delocalization, clearly seen in figure 5(*d*). This radically different behaviour can be understood by looking at wavefunctions (6) and (11) for the ξ- and η-coordinates, respectively. The only difference between equation (6) and the unperturbed wavefunction (3*a*) is that ξ/n is replaced by ξ/ϵ, where, in the strong-shift regime, ϵ is considerably larger than n. From this it follows that the wavefunction is stretched in the positive ξ-direction and therefore extends towards larger z-values.

In the η-coordinate an opposite effect occurs. The number of zeros in the wavefunction does not change by taking into account the boundary but the extension of the wavefunction is now limited to a smaller range in η. Therefore, in the η-coordinate the wavefunction is squeezed in such a way that all oscillations fit into the space available in the η-direction. In summary, the effect of the boundary is a stretching of the wavefunction in the ξ-direction and a squeezing in the η-direction. This explains the localization in the case $n_1 > n_2$ and the delocalization in the case $n_1 < n_2$.

Finally, we want to give some numbers in order to demonstrate in which situations the boundary becomes important. For this purpose we consider an atom initially in the parabolic eigenstate $n_1 = 0$, $n_2 = 60$ and $m = 0$, i.e. with quantum number $n = 61$. It turns out that an electron in this state acquires an $\epsilon \approx 100$ when the boundary is at $\eta_0 = 10^4$ (Bohr radii). This means that an atom in such a Rydberg state starts to feel the boundary when it is at

distances of the order of 1 μm.

3.5. Permanent dipole moments

It is a property of the parabolic eigenstates of hydrogen that they possess a permanent dipole moment [89]. Indeed, this property explains why these coordinates are so useful in describing the Stark effect [89] The dipole moment has zero x- and y-components and only the z-component is non-vanishing

$$e\langle z\rangle = \tfrac{3}{2}ea_0 n(n_1 - n_2).$$

In free space there are n^2 degenerate levels which can be superposed in such a way as to obtain an energy eigenstate with vanishing permanent dipole moment. For example, the spherical eigenstates do not possess a permanent dipole moment and they can be decomposed in parabolic eigenstates. When we take into account the paraboloidal boundary condition we break the symmetry of the system with respect to the x-y-plane and the atom acquires a permanent dipole moment. Because of the level splitting it is no longer possible to superpose degenerate eigenstates in order to obtain an eigenstate without permanent dipole moment.

For the strong-shift regime discussed in section 3.3 it is possible to calculate the expectation value of z exactly by making use of the wavefunction (13) and its normalization (14). In the appendix we find the result

$$\begin{aligned}\langle z\rangle = \Bigg\{&\epsilon^2[6n_1(n_1+|m|+1)+(|m|+1)(|m|+2)]\\ &-\eta_0^2\left(\frac{1}{10}+\frac{2(|m|^2-4)}{15j^2_{|m|,n_2}}+\frac{4(|m|^2-4)(|m|^2-1)}{15j^4_{|m|,n_2}}\right)\Bigg\}\\ &\times\left[4\epsilon\tilde{n}_1+4\eta_0\left(\frac{1}{6}+\frac{|m|^2-1}{3j^2_{|m|,n_2}}\right)\right]^{-1}. \qquad (15)\end{aligned}$$

In figure 6 we plot $\langle z\rangle$ for an atom in free space and for the case with a boundary at $\eta_0 = 100$. It can clearly be seen that the permanent dipole moments with the paraboloidal boundary are up to one order of magnitude larger than without the boundary. This effect occurs because the electron cloud is pushed in the positive z-direction due to the presence of the boundary.

4. A WKB-analysis

The preceding section was devoted to the problem of a hydrogen atom confined to the inside of a paraboloid. We have presented an implicit analytical solution and, in particular, have considered the case which is most interesting: when the energy levels are strongly shifted—the so-called strong-shift regime. For this regime we have found explicit analytical solutions for the wavefunctions, the eigenenergies, and also for the permanent dipole moments. It is desirable to obtain explicit analytical solutions also for the lower energy regime. From this we could learn more about the transition into the strong-shift regime. It is the purpose of this section to present a semiclassical calculation of the spectrum using the WKB-approximation and to simultaneously illuminate the underlying physics.

We start by recalling the differential equations of the preceding section and transforming them into a suitable form for the semiclassical treatment. We then apply in a 'naive' way the WKB-approximation to the problem with the paraboloidal boundary and show that it leads to inconsistencies under certain conditions. An improved semiclassical treatment enables

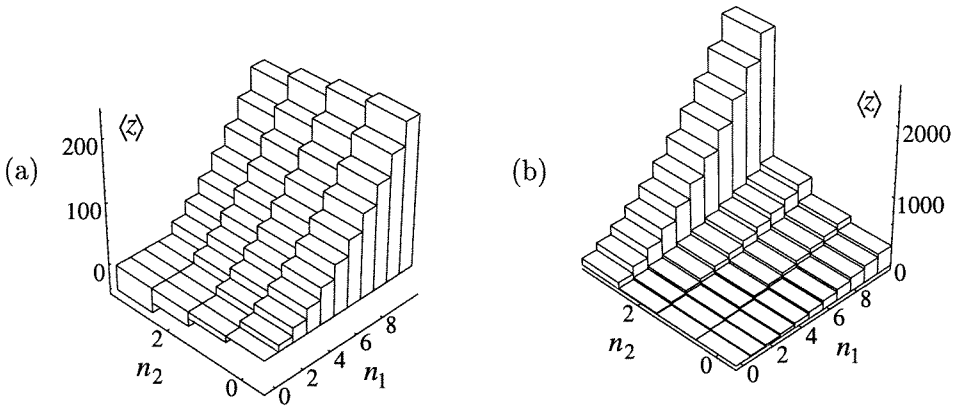

Figure 6. Permanent dipole moments of parabolic eigenstates with $m = 5$ (a) in free space and (b) with a paraboloidal boundary at $\eta_0 = 100$. Note the different scales on the vertical axes.

us to remove the inconsistencies of the naive approach and to present the correct Bohr–Sommerfeld quantization rule which is appropriate for our problem. Finally, we give a criterion which allows one to decide whether a specific level is considerably shifted due to the boundary or not.

4.1. Formulation of the problem

In the preceding section we have found the equations

$$\partial_\xi \xi \partial_\xi f_1 + \left(-\frac{1}{4\epsilon^2}\xi - \frac{m^2}{4\xi} + Z_1 \right) f_1 = 0 \tag{16a}$$

and

$$\partial_\eta \eta \partial_\eta f_2 + \left(-\frac{1}{4\epsilon^2}\eta - \frac{m^2}{4\eta} + Z_2 \right) f_2 = 0 \tag{16b}$$

determining the wavefunctions f_1 and f_2 corresponding to the ξ- and η-coordinates. As in the preceding section, Z_1 and Z_2 are the constants of separation satisfying the condition $Z_1 + Z_2 = 1$. We recall that in free space ϵ is an integer but this is no longer true for the case with the paraboloidal boundary. From equation (7) we know that

$$Z_2 = 1 - \frac{\tilde{n}_1}{\epsilon}$$

where

$$\tilde{n}_1 = n_1 + \tfrac{1}{2}|m| + \tfrac{1}{2}$$

and n_1 is a non-negative integer. This allows us to eliminate the separation constant Z_2 from equation (16b). We then find

$$f_2'' + \frac{1}{\eta} f_2' + \left(-\frac{1}{4\epsilon^2} + \frac{1 - \tilde{n}_1/\epsilon}{\eta} - \frac{m^2}{4\eta^2} \right) f_2 = 0.$$

We remove the first-order derivative term by putting

$$f_2(\eta) = \eta^{-1/2} w(\eta).$$

For $w(\eta)$ we obtain the 'Schrödinger equation'

$$w''(\eta) + \left(-\frac{1}{4\epsilon^2} - \tilde{V}(\eta)\right) w(\eta) = 0 \tag{17}$$

with the effective potential

$$\tilde{V}(\eta) = -\frac{1-\tilde{n}_1/\epsilon}{\eta} + \frac{m^2-1}{4\eta^2}.$$

Note that this potential depends via ϵ on the energy.

For a WKB treatment of the differential equation (17) it is necessary to modify the effective potential in the following way

$$V(\eta) = -\frac{1-\tilde{n}_1/\epsilon}{\eta} + \frac{m^2}{4\eta^2}. \tag{18}$$

An analogous procedure is well known in the WKB treatment of the hydrogen atom in spherical coordinates where the centrifugal term $l(l+1)/r^2$ is replaced by $(l+\frac{1}{2})^2/r^2$. This is the so-called *Langer-modification* [90] although it was suggested earlier by Kramers [91]. For a thorough discussion of it see, e.g. [92]. The reason for this is the singularity of the potential at the origin. Note that the exact result is also obtained without this replacement using supersymmetric WKB [93].

The momentum of the electron in this potential is given by

$$p(\eta) = \sqrt{-\frac{1}{4\epsilon^2} - V(\eta)}.$$

The classical turning points $\eta_\pm$ satisfy the condition $p(\eta_\pm) = 0$ and with the potential (18) turn out to be

$$\eta_\pm = 2\epsilon^2\left(1 - \frac{\tilde{n}_1}{\epsilon}\right) \pm 2\epsilon^2\sqrt{\left(1-\frac{\tilde{n}_1}{\epsilon}\right)^2 - \frac{m^2}{4\epsilon^2}}. \tag{19}$$

By using the relations

$$\eta_+\eta_- = \epsilon^2 m^2$$
$$\eta_+ + \eta_- = 4\epsilon^2(1-\tilde{n}_1/\epsilon)$$

we can write the square of the momentum in the simple form

$$p^2(\eta) = -\frac{1}{4\epsilon^2} - V(\eta) = \frac{1}{(2\epsilon\eta)^2}(\eta_+ - \eta)(\eta - \eta_-).$$

To write down the WKB solution we need the integral

$$\int_{\eta_-}^{\eta} p(\eta')\,\mathrm{d}\eta' = \frac{1}{2\epsilon}\int_{\eta_-}^{\eta}\frac{1}{\eta'}\sqrt{(\eta_+ - \eta')(\eta' - \eta_-)}\,\mathrm{d}\eta'$$

which yields

$$\int_{\eta_-}^{\eta} p(\eta')\,\mathrm{d}\eta' = \frac{1}{2\epsilon}\left[\sqrt{(\eta_+-\eta)(\eta-\eta_-)} + \frac{\eta_+ + \eta_-}{2}\arcsin\frac{2\eta - \eta_+ - \eta_-}{\eta_+ - \eta_-}\right.$$
$$\left. -\sqrt{\eta_+\eta_-}\arcsin\frac{\eta_+ + \eta_- - 2\eta_+\eta_-/\eta}{\eta_+ - \eta_-} + \frac{\pi}{2}\left(\frac{\eta_+ + \eta_-}{2} - \sqrt{\eta_+\eta_-}\right)\right]. \tag{20}$$

We can recover the standard result for free space by taking the upper limit of integration equal to the right turning point η_+ and applying Bohr–Sommerfeld quantization

$$2\int_{\eta_-}^{\eta_+} p(\eta)\,\mathrm{d}\eta = \frac{\pi}{\epsilon}\left(\frac{\eta_+ + \eta_-}{2} - \sqrt{\eta_+\eta_-}\right) \stackrel{!}{=} 2\pi\left(n_2 + \frac{1}{2}\right) \qquad n_2 = 0, 1, 2, \ldots.$$

This leads to the result

$$\epsilon = n_1 + n_2 + |m| + 1$$

which coincides with the exact result (5) of the full quantum calculation.

4.2. Naive WKB-approximation

We now concentrate on the case with the paraboloidal boundary. Whether or not there is a shift of the energy levels in a naive WKB picture depends on the value of the energy under consideration as is shown in figure 7. If the energy is small enough such that $\eta_+ < \eta_0$ then in a classical picture the electron does not feel the boundary and, therefore, there will be no considerable shift of the energy level:

$$\epsilon = n_1 + n_2 + |m| + 1 \qquad \text{for } \eta_+ < \eta_0. \tag{21}$$

However, for sufficiently high excited states, i.e. $\eta_0 < \eta_+$, the electron does reach the boundary and the energy levels in this regime are shifted considerably. In this case the usual Bohr–Sommerfeld quantization

$$\oint p \, \mathrm{d}\eta = 2\pi(n_2 + \tfrac{1}{2}) \tag{22}$$

must be modified because the WKB wavefunction

$$f_2(\eta) \approx \frac{1}{\sqrt{p(\eta)}} \sin\left(\int_{\eta_-}^{\eta} p \, \mathrm{d}\eta + \frac{\pi}{4} \right)$$

has to *vanish* at $\eta = \eta_0$, i.e.

$$\sin\left(\int_{\eta_-}^{\eta_0} p \, \mathrm{d}\eta + \frac{\pi}{4} \right) \stackrel{!}{=} 0$$

which leads to

$$2\int_{\eta_-}^{\eta_0} p \, \mathrm{d}\eta = 2\pi(n_2 + \tfrac{3}{4}). \tag{23}$$

From this and equation (20) we find

$$\begin{aligned} \epsilon = n_1 + n_2 + |m| + \frac{5}{4} - \frac{1}{2\pi\epsilon}\sqrt{(\eta_+ - \eta_0)(\eta_0 - \eta_-)} \\ + \frac{1}{\pi}\left(\epsilon - n_1 - \frac{1}{2}|m| - \frac{1}{2}\right) \arccos \frac{2\eta_0 - \eta_+ - \eta_-}{\eta_+ - \eta_-} \\ + \frac{|m|}{2\pi} \arccos \frac{\eta_+ + \eta_- - 2\eta_+\eta_-/\eta_0}{\eta_+ - \eta_-} \qquad \text{for } \eta_+ > \eta_0. \end{aligned} \tag{24}$$

Note that the right-hand side of this equation depends on ϵ explicitly as well as implicitly via $\eta_\pm(\epsilon)$. In order to find ϵ from this equation one must use numerical methods.

If we compare the two results (21) and (24) for the limiting case $\eta_0 \to \eta_+$ one finds two *different* results for ϵ, namely

$$\epsilon = n_1 + n_2 + |m| + 1 \qquad \text{(equation (21) for } \eta_0 \to \eta_+ -)$$

and

$$\epsilon = n_1 + n_2 + |m| + \tfrac{5}{4} \qquad \text{(equation (24) for } \eta_0 \to \eta_+ +).$$

This fact is due to an abrupt change in the Bohr–Sommerfeld quantization where the term $\frac{1}{2}$ of equation (22) is replaced by $\frac{3}{4}$ for higher energies. However, as we can now see,

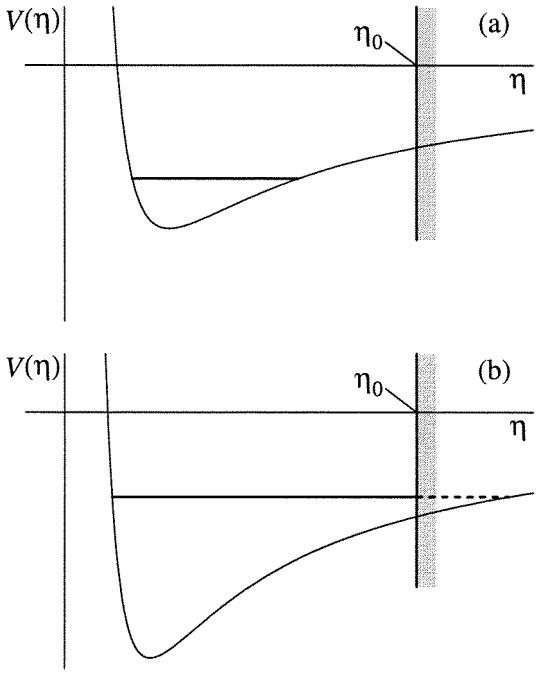

Figure 7. Level-shift and level-non-shift situation in a naive WKB picture. In (*a*) the considered energy is low enough so that the right turning point does not reach the boundary. In such a situation there will be no considerable shift of the energy level. In (*b*), however, the energy is high enough so that the right turning point does reach the boundary. This leads to a considerable shift of the energy level. Notice the energy dependence of the potential.

this abrupt change leads to unphysical results. Therefore, it is necessary to find a smooth transition between the two quantization rules of the form

$$\oint p \, \mathrm{d}\eta = 2\pi(n_2 + \tfrac{1}{2} + \delta(\epsilon)) \tag{25}$$

with an energy-dependent correction δ. In the limiting cases for small energies ($\eta_+ \ll \eta_0$) $\delta \approx 0$ and for high energies ($\eta_+ \gg \eta_0$) $\delta \approx \frac{1}{4}$. In the next section we will derive the function $\delta(\epsilon)$. We note that a similar modified quantization condition has been derived by Bestle *et al* [94] in the context of corner scattering of WKB waves. Friedrich and Trost [95, 96] proposed replacing the usual phase $\pi/4$ in the WKB wavefunction by a different value (depending on the potential under consideration) in cases where a wave is reflected from a potential. This can also lead to a modified quantization formula as in (25).

4.3. Improved WKB-approximation

The procedure for deriving the function δ is as follows. First we linearize the potential (18) around $\hat{\eta} \equiv \min(\eta_0, \eta_+)$. Then we solve equation (17) with the linearized potential exactly in terms of Airy functions. By writing this exact solution in a semiclassical approximation and comparing it with the WKB solution of the linearized potential we find the function δ. This procedure leads to expressions which are slightly different for the two cases $\eta_+ > \eta_0$ and $\eta_0 > \eta_+$. Therefore, it is necessary to treat them separately.

4.3.1. Right turning point beyond the wall: $\eta_+ > \eta_0$. In this case we linearize the potential around $\hat{\eta} = \eta_0$ and find

$$V_{\text{lin}}(\eta) = V(\eta_0) + V'(\eta_0)(\eta - \eta_0) = V_0 + V_0' \cdot (\eta - \eta_0)$$

where we have abbreviated $V'(\eta_0)$ by V_0'. The exact solution of the equation

$$w''(\eta) - \left(V_0 + V_0' \cdot (\eta - \eta_0) + \frac{1}{4\epsilon^2}\right) w(\eta) = 0$$

with the boundary condition $w(\eta_0) = 0$ reads

$$w(\eta) = \alpha_0 \,\text{Ai}\left[-V_0'^{1/3}\left(\eta_0 - \eta - \frac{V_0 + \frac{1}{4\epsilon^2}}{V_0'}\right)\right] - \alpha_0 q_0 \,\text{Bi}\left[-V_0'^{1/3}\left(\eta_0 - \eta - \frac{V_0 + \frac{1}{4\epsilon^2}}{V_0'}\right)\right]$$

where

$$q_0 \equiv \frac{\text{Ai}\left[\left(V_0 + \frac{1}{4\epsilon^2}\right) V_0'^{-2/3}\right]}{\text{Bi}\left[\left(V_0 + \frac{1}{4\epsilon^2}\right) V_0'^{-2/3}\right]}. \tag{26}$$

α_0 is an arbitrary constant and Ai and Bi denote the two independent Airy functions. Both of them are solutions of the differential equation $w'' - zw = 0$ and have an oscillatory behaviour for real, negative argument. Whereas Ai decays exponentially for real, positive argument, Bi increases exponentially.

Since the argument of the Airy functions is negative we can use the asymptotic expansions

$$\left.\begin{aligned} \text{Ai}(z) &\approx \frac{|z|^{-1/4}}{\sqrt{\pi}} \sin\left(\frac{2}{3}|z|^{3/2} + \frac{\pi}{4}\right) \\ \text{Bi}(z) &\approx \frac{|z|^{-1/4}}{\sqrt{\pi}} \cos\left(\frac{2}{3}|z|^{3/2} + \frac{\pi}{4}\right) \end{aligned}\right\} \qquad \text{for } |z| \gg 1,\ z < 0$$

and find

$$w(\eta) \sim \sin\left[\frac{2}{3} V_0'^{1/2}\left(\eta_0 - \eta - \frac{V_0 + \frac{1}{4\epsilon^2}}{V_0'}\right)^{3/2} + \frac{\pi}{4} - \text{Arctan}\, q_0\right]. \tag{27}$$

Here Arctan denotes the multivalued inverse function of tan, i.e. $\text{Arctan}\, q_0 = \arctan q_0 + \nu\pi$, where arctan denotes the principal branch and ν is an integer.

On the other hand, we can directly write down the WKB solution for the linearized potential. The oscillating part of it reads

$$\begin{aligned} \sin\left(\int_{\eta_-}^{\eta} p \,\mathrm{d}\eta + \frac{\pi}{4}\right) &= \sin\left(\int_{\eta_-}^{\eta_0} p \,\mathrm{d}\eta - \int_{\eta}^{\eta_0} p \,\mathrm{d}\eta + \frac{\pi}{4}\right) \\ &\approx \sin\left(\int_{\eta_-}^{\eta_0} p \,\mathrm{d}\eta - \int_{\eta}^{\eta_0} \sqrt{-\frac{1}{4\epsilon^2} - V_{\text{lin}}(\eta)}\,\mathrm{d}\eta + \frac{\pi}{4}\right) \\ &= -\sin\left[-\int_{\eta_-}^{\eta_0} p \,\mathrm{d}\eta + \frac{2}{3} V_0'^{1/2}\left(\eta_0 - \eta - \frac{V_0 + \frac{1}{4\epsilon^2}}{V_0'}\right)^{3/2}\right. \\ &\quad \left. -\frac{2}{3V_0'}\left(-\frac{1}{4\epsilon^2} - V_0\right)^{3/2} - \frac{\pi}{4}\right]. \end{aligned}$$

This expression has to equal equation (27) which leads to

$$2\int_{\eta_-}^{\eta_0} p\,\mathrm{d}\eta = 2\pi\left(n_2+\frac{1}{2}\right)+2\,\mathrm{Arctan}\,q_0-\frac{2}{3V_0'}\left(-\frac{1}{4\epsilon^2}-V_0\right)^{3/2}$$
$$=2\pi\left(n_2+\frac{1}{2}+\delta_0\right)$$

where n_2 is a positive integer or zero and the correction δ_0 is defined by

$$\delta_0=\frac{1}{\pi}\,\mathrm{Arctan}\,q_0-\frac{2}{3\pi}\frac{1}{V_0'}\left(-\frac{1}{4\epsilon^2}-V_0\right)^{3/2}. \tag{28}$$

Let us discuss the special case $\eta_+\gg\eta_0\gg 1$. Then from equation (18) we can estimate $V_0\approx -1/\eta_0$ and $V_0'\approx 1/\eta_0^2$ and hence $|V_0/V_0'^{2/3}|\approx\eta_0^{1/3}\gg 1$. Thus we can use the asymptotic expansions for the Airy functions in (26) and find

$$q_0\approx\tan\left[\frac{2}{3}\left(-\frac{V_0+\frac{1}{4\epsilon^2}}{V_0'^{2/3}}\right)^{3/2}+\frac{\pi}{4}\right].$$

We therefore obtain the correction $\delta_0=\frac{1}{4}$. Substituting this result into equation (25) shows perfect agreement with equation (23).

Another special case is $\eta_+=\eta_0$. Then $q_0=\mathrm{Ai}(0)/\mathrm{Bi}(0)=1/\sqrt{3}$ and

$$\delta_0(\epsilon_c)=\frac{1}{\pi}\,\mathrm{Arctan}\,q_0=\frac{1}{6}. \tag{29}$$

4.3.2. Wall beyond the right turning point: $\eta_0>\eta_+$. In this case we linearize the potential around $\hat{\eta}=\eta_+$ and find

$$V_{\mathrm{lin}}(\eta)=V(\eta_+)+V'(\eta_+)(\eta-\eta_+)=V_++V_+'\cdot(\eta-\eta_+)$$

where we have abbreviated $V'(\eta_+)$ by V_+'. The exact solution of the equation

$$w''(\eta)-\left(V_++V_+'\cdot(\eta-\eta_+)+\frac{1}{4\epsilon^2}\right)w(\eta)=0$$

with the boundary condition $w(\eta_0)=0$ reads

$$w(\eta)=\alpha_+\,\mathrm{Ai}[V_+'^{1/3}\cdot(\eta-\eta_+)]-\alpha_+q_+\,\mathrm{Bi}[V_+'^{1/3}\cdot(\eta-\eta_+)]$$

where

$$q_+\equiv\frac{\mathrm{Ai}[V_+'^{1/3}\cdot(\eta_0-\eta_+)]}{\mathrm{Bi}[V_+'^{1/3}\cdot(\eta_0-\eta_+)]} \tag{30}$$

and α_+ is an arbitrary constant. Again we use the asymptotic expressions for the Airy functions and find

$$w(\eta)\sim\sin\left[\frac{2}{3}\,V_+'^{1/2}(\eta_+-\eta)^{3/2}+\frac{\pi}{4}-\mathrm{Arctan}\,q_+\right]. \tag{31}$$

On the other hand, the WKB solution for the linearized potential has the oscillatory part

$$\sin\left(\int_{\eta_-}^{\eta}p\,\mathrm{d}\eta+\frac{\pi}{4}\right)=\sin\left(\int_{\eta_-}^{\eta_+}p\,\mathrm{d}\eta-\int_{\eta}^{\eta_+}p\,\mathrm{d}\eta+\frac{\pi}{4}\right)$$
$$\approx\sin\left(\int_{\eta_-}^{\eta_+}p\,\mathrm{d}\eta-\int_{\eta}^{\eta_+}\sqrt{-\frac{1}{4\epsilon^2}-V_{\mathrm{lin}}(\eta)}\,\mathrm{d}\eta+\frac{\pi}{4}\right)$$
$$=-\sin\left(\int_{\eta_-}^{\eta_+}p\,\mathrm{d}\eta+\frac{2}{3}V_+'^{1/2}(\eta_+-\eta)^{3/2}-\frac{\pi}{4}\right).$$

This must equal equation (31) which leads to

$$2\int_{\eta_-}^{\eta_+} p\,\mathrm{d}\eta = 2\pi(n_2+\tfrac{1}{2}) + 2\,\mathrm{Arctan}\,q_+ = 2\pi(n_2+\tfrac{1}{2}+\delta_+)$$

where we have defined

$$\delta_+ = \frac{1}{\pi}\,\mathrm{Arctan}\,q_+. \tag{32}$$

For the case $\eta_0 \gg \eta_+$ we already know that the correction δ_+ must be very small. Indeed, the argument of the Airy functions in (30) is large and positive and, therefore, q_+ is exponentially small. It follows that in (32) we must have $\mathrm{Arctan}\,q_+ = \arctan q_+$, i.e. $\nu = 0$, in order to have $\delta_+ = 0$ which together with (25) agrees with (22). The other special case is $\eta_0 = \eta_+$ which again yields $\delta_+ = \frac{1}{6}$. This shows that the transition from $\eta_0 > \eta_+$ to $\eta_0 < \eta_+$ no longer produces an abrupt change in the quantization rule.

A subtle point remains to be discussed concerning the multivalued function $\mathrm{Arctan}\,q_0 = \arctan q_0 + \nu\pi$ and how to determine the correct integer ν.

4.3.3. Discussion of $\mathrm{Arctan}\,q_0$. In order to understand the meaning of $\mathrm{Arctan}\,q_0$ in our context it is best to consider a situation with fixed η_0 and variable η_+ (or energy parameter ϵ). Let us start with a value of ϵ such that $\eta_+ \ll \eta_0$. In this case the argument of the Airy function in (30) is exponentially small. For $\eta_+ \ll \eta_0$ there must not be any phase shift at all and, therefore, we have to take the principal branch of Arctan as already discussed in the preceding section. Now we increase ϵ up to the value where $\eta_+ = \eta_0$. In this case the argument of the Airy function vanishes and $q_+ = q_0 = 1/\sqrt{3}$. We still have to take the principal branch of Arctan and obtain the correction $\delta = \frac{1}{6}$. We increase ϵ further. Now we have to consider the Airy functions of (26). Their argument is negative and hence both nominator and denominator are oscillatory functions. For a certain value of ϵ the function Bi vanishes for the first time. Just before that, the argument of Arctan is ∞ and its (principal) value is $\pi/2$. Just after the first zero of Bi, the argument of Arctan is $-\infty$. The correction δ should be a continuous function which, at this point, requires $\mathrm{Arctan}(-\infty) = \arctan(-\infty) + 1\cdot\pi = -\pi/2 + \pi = \pi/2$. This means that we have to jump to the next branch of Arctan. This happens at all zeros of Bi.

4.4. The unified quantization rule

We are now in a position to unify, at least formally, the quantization rules for the two cases discussed in sections 4.3.1 and 4.3.2. For this purpose it is convenient to introduce

$$\mathcal{V}(\hat\eta) \equiv \frac{1}{(2\epsilon)^{2/3}}\,\frac{(\eta_0-\eta_+)(\hat\eta-\eta_-)}{[\eta_+(\hat\eta-\eta_-)-\eta_-(\eta_+-\hat\eta)]^{2/3}}.$$

With the convention $\hat\eta \equiv \min(\eta_0,\eta_+)$ one can verify that

$$q = \frac{\mathrm{Ai}\,\mathcal{V}(\hat\eta)}{\mathrm{Bi}\,\mathcal{V}(\hat\eta)}$$

is identical to q_0 and q_+, respectively, depending on whether $\hat\eta = \eta_0$ or $\hat\eta = \eta_+$. With these definitions we can formulate the unified quantization rule as

$$\oint p\,\mathrm{d}\eta = 2\int_{\eta_-}^{\hat\eta} p\,\mathrm{d}\eta = 2\pi(n_2+\tfrac{1}{2}+\delta(\hat\eta))$$

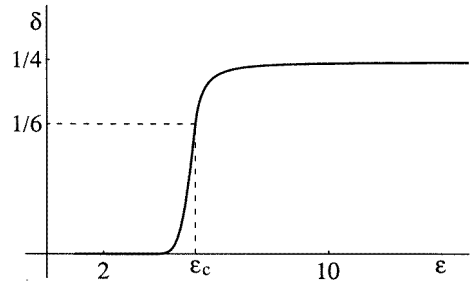

Figure 8. Example for the correction function δ, equation (33), for $n_1 = 0$, $m = 0$ and $\eta_0 = 100$.

where

$$\delta(\hat{\eta}) = \frac{1}{\pi}\arctan\frac{\mathrm{Ai}\,\mathcal{V}(\hat{\eta})}{\mathrm{Bi}\,\mathcal{V}(\hat{\eta})} + \nu - \frac{2}{3\pi}\theta(\eta_+ - \eta_0)|\mathcal{V}(\hat{\eta})|^{3/2}. \tag{33}$$

Here ν is the number of zeros of $\mathrm{Bi}\,\mathcal{V}(\hat{\eta})$ between $\mathcal{V}(\hat{\eta})$ and 0, and θ denotes the unit step function. Figure 8 shows the correction δ as a function of ϵ for a specific choice of n_1, m, and η_0.

The question which remains to be answered is how to fix $\hat{\eta}$, i.e. how to decide in advance whether $\hat{\eta} = \eta_+$ or $\hat{\eta} = \eta_0$ for given n_1, n_2, m, and η_0. This problem will be discussed in the next section.

4.5. A criterion for level shift

Finding out which value to choose for $\hat{\eta}$, at the same time answers the question whether a given level specified by n_1, n_2, and m is shifted when one requires the wavefunction to vanish at η_0. The reason is as follows. If it turns out that $\hat{\eta} = \eta_+$, i.e. $\min(\eta_0, \eta_+) = \eta_+$ or $\eta_+ < \eta_0$, then according to our naive WKB approach of section 4.2 there is no shift at all and the improved WKB method predicts only a slight shift. On the other hand, when $\hat{\eta} = \eta_0$ then classically the electron bounces against the boundary and a considerable shift of the energy level is expected.

For the following it will be useful to define a critical value of ϵ by

$$\eta_+(\epsilon = \epsilon_c) = \eta_0.$$

Hence, $\epsilon = \epsilon_c$ corresponds to a situation where the right turning point exactly reaches the boundary. Note that ϵ_c depends on n_1, m, and, of course, on η_0. Using equation (19) for $\eta_\pm$ we obtain

$$\epsilon_c = \frac{2\eta_0\tilde{n}_1 + \eta_0\sqrt{4\tilde{n}_1^2 + 4\eta_0 - m^2}}{4\eta_0 - m^2}.$$

However, ϵ_c actually is the solution of $\eta_0 = \eta_\pm(\epsilon)$ because we had to take the square while solving this equation. Whether $\eta_+(\epsilon_c) = \eta_0$ or $\eta_-(\epsilon_c) = \eta_0$ depends on $|m|$ and n_1. ϵ_c switches from $\eta_+ = \eta_0$ to $\eta_- = \eta_0$ when $\eta_+ = \eta_-$. Physically this means that the minimum of the potential lies exactly at $\eta = \eta_0$. This behaviour defines a critical value for $|m|$ (depending on n_1) which turns out to be

$$|m|_c = \tfrac{1}{2}\sqrt{(n_1 + \tfrac{1}{2})^2 + 4\eta_0} - \tfrac{1}{2}(n_1 + \tfrac{1}{2}).$$

In figure 9 we demonstrate some typical cases and the role of ϵ_c and $|m|_c$. For $0 \leqslant |m| \leqslant |m|_c$ there are some levels which are almost unshifted, that is, for some values

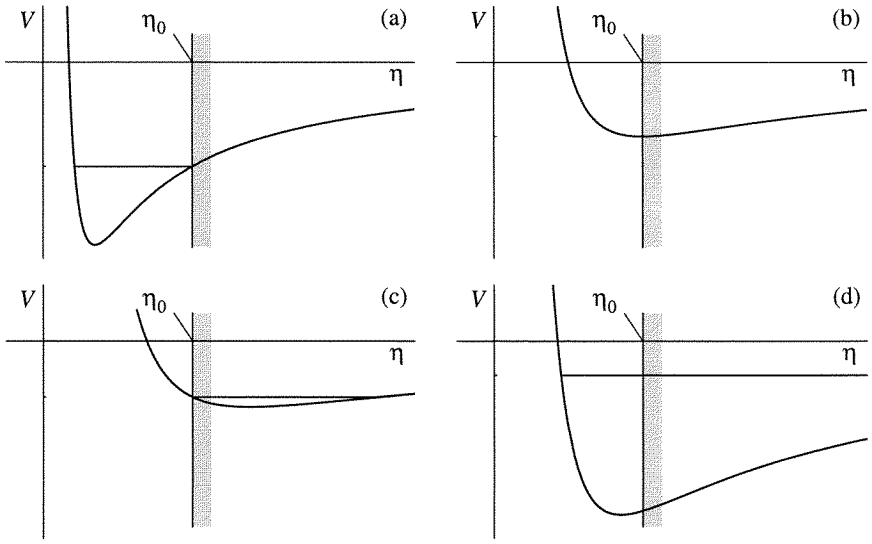

Figure 9. Interplay between the critical values ϵ_c and $|m|_c$. (*a*) $\epsilon = \epsilon_c$, $0 \leqslant |m| \leqslant |m|_c$. The energy is chosen in such a way that the right turning point exactly reaches the boundary. There may be some unshifted levels with $\epsilon < \epsilon_c$. (*b*) $\epsilon = \epsilon_c$, $|m| = |m|_c$. In this case the left and right turning points are identical and equal to η_0. This defines the critical value of $|m|$. (*c*) $\epsilon = \epsilon_c$, $|m| > |m|_c$. Here no unshifted levels can exist. Depending on the value of $|m|$ there may be some strongly shifted levels. (*d*) $\epsilon > \epsilon_c$, $|m|_{max} > |m| > |m|_c$. For values of ϵ larger than ϵ_c the minimum of the effective potential moves a little bit towards smaller values of η. As long as $|m|$ is smaller than $|m|_{max}$ there exist some levels which are strongly shifted.

$n_2 = 0, 1, 2, \ldots, (n_2)_c$ we have $\hat{\eta} = \eta_+$. The value $(n_2)_c$ is reached for $\eta_+ = \eta_0$. In this specific situation we have

$$2\int_{\eta_-}^{\eta_+} p(\eta)\,\mathrm{d}\eta = 2\pi((n_2)_c + \tfrac{1}{2} + \delta(\epsilon_c))$$

or together with equation (29)

$$\epsilon_c - n_1 - |m| - \tfrac{1}{2} = (n_2)_c + \tfrac{1}{2} + \tfrac{1}{6}.$$

This yields

$$(n_2)_c = \epsilon_c - n_1 - |m| - \tfrac{7}{6} \qquad \text{for } |m| < |m|_c.$$

The number of levels with energy less than zero in the potential (18) with a boundary at $\eta = \eta_0$ is finite. Therefore, there exists a maximum for the quantum number n_2, denoted by $(n_2)_{max}$. Its value can be derived by taking the limit $\epsilon \to \infty$ of equation (24) and solving for n_2. The calculation leads to the result

$$(n_2)_{max} = \frac{1}{\pi}\sqrt{4\eta_0 - m^2} - \frac{|m|}{\pi}\arccos\frac{|m|}{2\sqrt{\eta_0}} - \frac{3}{4}.$$

Note that $(n_2)_{max}$ does not depend on the quantum number n_1. For all n_2 with $(n_2)_c < n_2 < (n_2)_{max}$ the corresponding levels are considerably shifted. It might occur that $(n_2)_{max} = 0$. This defines a maximum value of $|m|$ since for larger values of $|m|$, $(n_2)_{max}$ becomes negative and there are no bound states at all. Unfortunately, $|m|_{max}$ cannot be calculated analytically but must be found numerically as the solution of the transcendental equation

$$\frac{1}{\pi}\sqrt{4\eta_0 - |m|_{max}^2} - \frac{|m|_{max}}{\pi}\arccos\frac{|m|_{max}}{2\sqrt{\eta_0}} = \frac{3}{4}.$$

Table 1. This table serves as a guide how to determine $\hat{\eta}$ for given values of $|m|$ and n_2.

$\lvert m\rvert$	n_2	$\hat{\eta}$
	$0 \leqslant n_2 \leqslant (n_2)_c$	η_+
$0 \leqslant \lvert m\rvert \leqslant \lvert m\rvert_c$	$(n_2)_c < n_2 < (n_2)_{max}$	η_0
$\lvert m\rvert_c < \lvert m\rvert \leqslant \lvert m\rvert_{max}$	$n_2 = 0, 1, 2, \ldots, (n_2)_{max}$	η_0
$\lvert m\rvert > \lvert m\rvert_{max}$	$n_2 = 0, 1, 2, \ldots$	no bound states

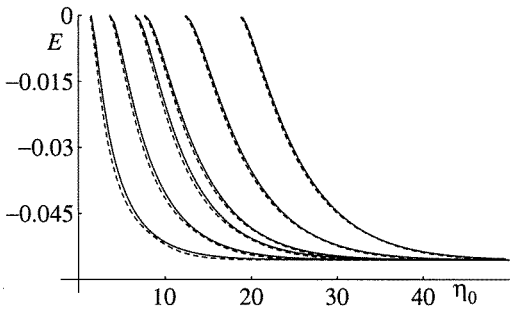

Figure 10. Comparison of the improved WKB calculations with the exact result. Here we plot the dependence of the $n = 3$ levels for free hydrogen on η_0. The agreement of the two results is very good.

An upper limit for $|m|_{max}$ is given by

$$|m|_{max} < 2\sqrt{\eta_0}.$$

Table 1 summarizes the results of this section and serves as a guide for the determination of $\hat{\eta}$.

In figure 10 we compare the result of the semiclassical calculation with the exact result of the preceding section and find an excellent agreement between the two results.

The fact that the effective potential for the motion in the η-direction depends on the energy, makes it necessary to introduce the critical and maximum values of $|m|$ and n_2 and to distinguish all the different cases as we have done it. However, once this is established one can easily predict whether an arbitrary level specified by the quantum numbers n_1, n_2, and m is shifted or not.

We conclude this section by noting that the WKB solution not only highlights the underlying physics of the problem but also is very useful for the determination of approximate energy eigenvalues and eigenfunctions. It is an advantage of the semiclassical method that the quantum numbers of the solution can be specified in advance. The semiclassical solution which is obtained for these specific quantum numbers can then be used as a starting point for a purely numerical method.

5. Summary

In this paper we have presented a brief history of confined quantum systems, in particular, we have summarized the work which has been done on confined atoms, molecules, harmonic oscillators and a few other systems. We have also described the theoretical methods which have been used for treating these systems. We then concentrated on the hydrogen atom as our model system and discussed the separability of the hydrogenic Schrödinger equation

in various coordinate systems. We chose the parabolic coordinates for our studies and considered a hydrogen atom confined to a space with a paraboloidal boundary where the nucleus of the atom is fixed at the focus of the paraboloid. We have derived an exact implicit analytical solution for the energy eigenvalues of the bound states and for the wavefunctions. In the case where the energy levels are strongly shifted compared with a free atom—in the so-called strong-shift regime—we have also found explicit solutions for the eigenenergies and the eigenfunctions. In the last section we have applied semiclassical methods in order to gain deeper insight into the physics of the problem. Finally, we have derived a modified Bohr–Sommerfeld quantization rule which allows us to calculate the energy eigenvalues from a transcendental equation with a very good accuracy.

Acknowledgments

We are grateful to M M Nieto for many helpful comments and for drawing our attention to some useful references. VPY acknowledges support by the Heraeus Foundation and the Russian Foundation for Basic Research, and DSK acknowledges support by the Deutsche Forschungsgemeinschaft.

Appendix. Calculations for the strong-shift regime

In this appendix we perform some calculations needed in connection with the strong-shift regime. We first set up some auxiliary formulae needed for the calculation, then we calculate the normalization constant of the wavefunction (13) and finally we work out the expection value of the z-coordinate.

A.1. Auxiliary formulae

Using the orthogonality relation for the Laguerre polynomials [88]

$$\int_0^\infty x^\alpha \mathrm{e}^{-x} L_j^\alpha(x) L_k^\alpha(x)\,\mathrm{d}x = \frac{\Gamma(\alpha+j+1)}{j!}\delta_{jk} \tag{A1}$$

and the recurrence relation

$$(n+1)L_{n+1}^\alpha(x) - (2n+\alpha+1-x)L_n^\alpha(x) + (n+\alpha)L_{n-1}^\alpha(x) = 0$$

we find

$$\int_0^\infty x^{|m|+1}\mathrm{e}^{-x}[L_{n_1}^{|m|}(x)]^2\,\mathrm{d}x = (2n_1+|m|+1)\frac{(n_1+|m|)!}{n_1!} \tag{A2}$$

and

$$\int_0^\infty x^{|m|+2}\mathrm{e}^{-x}[L_{n_1}^{|m|}(x)]^2\,\mathrm{d}x = [(2n_1+|m|+1)^2 + (n_1+1)((n_1+|m|+1)+n_1(n_1+|m|)]\frac{(n_1+|m|)!}{n_1!}. \tag{A3}$$

We will also need several integrals of the type

$$\int_0^1 x^\lambda J_\nu^2(\alpha x)\,\mathrm{d}x.$$

For our purposes λ has the values 1, 3 and 5. These integrals can be calculated recursively using formulae 1.8.3.4

$$\int x^\lambda J_\nu^2(x)\,\mathrm{d}x = \frac{\lambda-1}{\lambda}\left(\nu^2-\frac{(\lambda-1)^2}{4}\right)\int x^{\lambda-2}J_\nu^2(x)\,\mathrm{d}x + \frac{x^{\lambda-1}}{2\lambda}\left\{\left[xJ_\nu'(x)-\frac{\lambda-1}{2}J_\nu(x)\right]^2+\left[x^2-\nu^2+\frac{(\lambda-1)^2}{4}\right]J_\nu^2(x)\right\}$$

and 1.8.3.11

$$\int_0^x xJ_\nu(\alpha x)\,\mathrm{d}x = \frac{x^2}{2}\left[J_\nu'(\alpha x)\right]^2+\frac{1}{2}\left(x^2-\frac{\nu^2}{\alpha^2}\right)J_\nu^2(\alpha x)$$

of [97]. In our case α is a zero of $J_\nu(x)$ and, therefore, the integrals can be simplified significantly by using the relation [88]

$$J_\nu'(x) = -J_{\nu+1}(x)+\frac{\nu}{x}J_\nu(x).$$

This finally leads to the formulae

$$\int_0^1 xJ_\nu^2(\alpha x)\,\mathrm{d}x = \tfrac{1}{2}J_{\nu+1}^2(\alpha) \tag{A4}$$

$$\int_0^1 x^3J_\nu^2(\alpha x)\,\mathrm{d}x = \left(\frac{1}{6}+\frac{\nu^2-1}{3\alpha^2}\right)J_{\nu+1}^2(\alpha) \tag{A5}$$

$$\int_0^1 x^5J_\nu^2(\alpha x)\,\mathrm{d}x = \left(\frac{1}{10}+\frac{2(\nu^2-4)}{15\alpha^2}+\frac{4(\nu^2-4)(\nu^2-1)}{15\alpha^4}\right)J_{\nu+1}^2(\alpha). \tag{A6}$$

A.2. Normalization of strong-shift wavefunction

In section 3 we found for the strong-shift regime the approximate wavefunction (13)

$$\tilde\psi_{n_1,n_2,m}(\xi,\eta,\varphi) = \tilde{\mathcal{N}}\xi^{\frac{1}{2}|m|}\exp\left(-\frac{\xi}{2\epsilon}\right)L_{n_1}^{|m|}(\xi/\epsilon)J_{|m|}\left(\sqrt{\eta/\eta_0}j_{|m|,n_2}\right)\mathrm{e}^{\mathrm{i}m\varphi}$$

where the energy parameter ϵ is given by equation (12). We now want to calculate the normalization constant $\tilde{\mathcal{N}}$. It is needed in order to evaluate matrix elements, for example the permanent dipole moments of the eigenstates in the strongly-shift regime.

In parabolic coordinates the volume element is given by $(\xi+\eta)/4$. Therefore, we have to calculate

$$1 = \int_0^{2\pi}\int_0^\infty\int_0^{\eta_0}|\tilde\psi_{n_1,n_2,m}(\xi,\eta,\varphi)|^2\frac{\xi+\eta}{4}\,\mathrm{d}\eta\,\mathrm{d}\xi\,\mathrm{d}\varphi = \tilde{\mathcal{N}}^2\frac{\pi}{2}\int_0^\infty\int_0^{\eta_0}\xi^{|m|}(\xi+\eta)\mathrm{e}^{-\xi/\epsilon}\left[L_{n_1}^{|m|}(\xi/\epsilon)\right]^2J_{|m|}^2\left(\sqrt{\eta/\eta_0}j_{|m|,n_2}\right)\mathrm{d}\eta\,\mathrm{d}\xi$$

where we have inserted the wavefunction (13) and performed integration over the azimuthal angle φ. After the substitution

$$x = \xi/\epsilon \qquad y = \sqrt{\eta/\eta_0}$$

and using equations (A1), (A2), (A4), and (A5) we end up with

$$1 = \tilde{\mathcal{N}}^2\pi\eta_0^2\epsilon^{|m|+1}\frac{(n_1+|m|)!}{n_1!}J_{|m|+1}^2(j_{|m|,n_2})\left(\frac{\epsilon}{\eta_0}\tilde n_1+\frac{1}{6}+\frac{|m|^2-1}{3j_{|m|,n_2}^2}\right)$$

which immediately gives the normalization constant (14).

A.3. Permanent dipole moments

In a similar manner we calculate the permanent dipole moments. This is essentially the expectation value of the z-coordinate since the x- and y-components vanish. Because

$$z = \frac{\xi - \eta}{2}$$

we have to calculate

$$\langle z \rangle = \int_0^{2\pi} \int_0^{\infty} \int_0^{\eta_0} \frac{\xi - \eta}{2} |\tilde{\psi}_{n_1,n_2,m}(\xi, \eta, \varphi)|^2 \frac{\xi + \eta}{4} \, \mathrm{d}\eta \, \mathrm{d}\xi \, \mathrm{d}\varphi$$
$$= \tilde{\mathcal{N}}^2 \frac{\pi}{4} \int_0^{\infty} \int_0^{\eta_0} \xi^{|m|} (\xi^2 - \eta^2) \mathrm{e}^{-\xi/\epsilon} [L_{n_1}^{|m|}(\xi/\epsilon)]^2 J_{|m|}^2 \left(\sqrt{\eta/\eta_0} j_{|m|,n_2} \right) \mathrm{d}\eta \, \mathrm{d}\xi .$$

Again we substitute

$$x = \xi/\epsilon \qquad y = \sqrt{\eta/\eta_0}$$

and employ the equations (A1), (A3), (A4), and (A6) and finally arrive at the result (15).

References

[1] You J H, Ye Z G and Du M L 1990 *Phys. Rev.* B **41** 8180
[2] Ley-Koo E and García-Castelán R M G 1991 *J. Phys. A: Math. Gen.* **24** 1481
[3] Krähmer D S 1997 *Dissertation* University of Ulm
[4] Michels A, de Boer J and Bijl A 1937 *Physica* **4** 981
[5] Sommerfeld A and Welker H 1938 *Ann. Phys.* **32** 56
[6] de Groot S R and ten Seldam C A 1946 *Physica* **12** 669
[7] ten Seldam C A and de Groot S R 1952 *Physica* **18** 891
[8] ten Seldam C A and de Groot S R 1952 *Physica* **18** 905
[9] Dingle R B 1953 *Proc. Camb. Phil. Soc.* **49** 103
[10] Perlson B D and Weil J A 1974 *J. Magn. Reson.* **15** 594
[11] Suryanarayana D and Weil J A 1976 *J. Chem. Phys.* **64** 510
[12] Ludeña E V 1976 *J. Chem. Phys.* **66** 468
[13] Weil J A 1979 *J. Chem. Phys.* **71** 2803
[14] Ley-Koo E and Rubinstein S 1980 *J. Chem. Phys.* **73** 887
[15] Ley-Koo E and Cruz S A 1981 *J. Chem. Phys.* **74** 603
[16] Goshen S, Friedman M, Thieberger R and Weil J A 1983 *J. Chem. Phys.* **79** 4363
[17] Wigner E P 1954 *Phys. Rev.* **94** 77
[18] Trees R E 1956 *Phys. Rev.* **102** 1553
[19] Gray B F 1962 *J. Chem. Phys.* **36** 1801
[20] Gray B F 1971 *J. Chem. Phys.* **55** 2848
[21] Gray B F and Gonda I 1975 *J. Chem. Phys.* **62** 2007
[22] Fowler P W 1984 *Mol. Phys.* **53** 865
[23] Ley-Koo E and Rubinstein S 1979 *J. Chem. Phys.* **71** 351
[24] Cruz S A, Ley-Koo E, Marín J L and Taylor-Armitage A 1995 *Int. J. Quantum Chem.* **54** 3
[25] Cottrell T L 1951 *Trans. Faraday Soc.* **47** 337
[26] Singh K K 1964 *Physica* **30** 211
[27] Marín J L and Muñoz G 1993 *J. Mol. Struct.* **287** 281
[28] LeSar R and Herschbach D R 1981 *J. Phys. Chem.* **85** 2798
[29] LeSar R and Herschbach D R 1983 *J. Phys. Chem.* **87** 5202
[30] Levine J D 1965 *Phys. Rev.* **140** A586
[31] Gadzuk J W 1967 *Phys. Rev.* **154** 662
[32] Liu Z and Lin D L 1983 *Phys. Rev.* B **28** 4413
[33] Satpathy S 1983 *Phys. Rev.* B **28** 4585
[34] Shan Y, Jiang T-F and Lee Y C 1985 *Phys. Rev.* B **31** 5487
[35] Shan Y 1987 *J. Phys. B: At. Mol. Phys.* **20** 4275

[36] Shan Y, Lu P-C and Tseng H C 1987 *J. Phys. B: At. Mol. Phys.* **20** 4285
[37] Kovalenko A F, Sovyak E N and Holovko M F 1989b *Phys. Status Solidi* **155** 549
[38] Shan Y 1990 *J. Phys. B: At. Mol. Opt. Phys.* **23** L1
[39] Kovalenko A F and Holovko M F 1992 *J. Phys. B: At. Mol. Opt. Phys.* **25** L233
[40] Kovalenko A F, Sovyak E N and Holovko M F 1992 *Int. J. Quantum Chem.* **42** 321
[41] Chandrasekhar S 1943 *Astrophys. J.* **97** 255
[42] Auluck F C and Kothari D S 1945 *Proc. Camb. Phil. Soc.* **41** 175
[43] Baijal J S and Singh K K 1955 *Prog. Theor. Phys.* **14** 214
[44] Dean P 1966 *Proc. Camb. Phil. Soc.* **62** 277
[45] Vawter R 1968 *Phys. Rev.* **174** 749
[46] Vawter R 1973 *J. Math. Phys.* **14** 1864
[47] Consortini A and Frieden B R 1976 *Nuovo Cimento* B **35** 153
[48] Rotbart F C 1978 *J. Phys. A: Math. Gen.* **11** 2363
[49] Aguilera-Navarro V C, Ley-Koo E and Zimerman A H 1980 *J. Phys. A: Math. Gen.* **13** 3585
[50] Aguilera-Navarro V C, Gomes J F, Zimerman A H and Ley-Koo E 1983 *J. Phys. A: Math. Gen.* **16** 2943
[51] Aquino N 1997 *J. Phys. A: Math. Gen.* **30** 2403
[52] Sommerfeld A and Hartmann H 1940 *Ann. Phys.* **37** 333
[53] Chaudhuri R N and Mukherjee B 1983 *J. Phys. A: Math. Gen.* **16** 3193
[54] Froehlich H 1938 *Phys. Rev.* **54** 945
[55] Berman D H 1991 *Am. J. Phys.* **59** 937
[56] Wassermann G D 1948 *Proc. Camb. Phil. Soc.* **44** 251
[57] Gonda I and Gray B F 1975 *J. Chem. Soc. Faraday Trans.* II **71** 2016
[58] Hull T E and Julius R S 1956 *Can. J. Phys.* **34** 914
[59] Gorecki J and Byers Brown W 1987 *J. Phys. B: At. Mol. Phys.* **20** 5953
[60] Gorecki J and Byers Brown W 1989 *J. Phys. B: At. Mol. Opt. Phys.* **22** 2659
[61] Marín J L and Cruz S A 1991 *J. Phys. B: At. Mol. Opt. Phys.* **24** 2899
[62] Marín J L and Cruz S A 1991 *Am. J. Phys.* **59** 931
[63] Marín J L, Rosas R and Uribe A 1995 *Am. J. Phys.* **63** 460
[64] Goodfriend P L 1990 *J. Phys. B: At. Mol. Opt. Phys.* **23** 1373
[65] Diamond J J, Goodfriend P L and Tsonchev S 1991 *J. Phys. B: At. Mol. Opt. Phys.* **24** 3669
[66] Brownstein K R 1993 *Phys. Rev. Lett.* **71** 1427
[67] Hirschfelder J O 1960 *J. Chem. Phys.* **33** 1462
[68] Swenson R J and Danforth S H 1972 *J. Chem. Phys.* **57** 1734
[69] Fernández F M and Castro E A 1981 *Int. J. Quantum Chem.* **19** 521
[70] Arteca G A, Maluendes S A, Fernández F M and Castro E A 1983 *Int. J. Quantum Chem.* **24** 169
[71] Inglesfield J E 1981 *J. Phys. C: Solid State Phys.* **14** 3795
[72] Crampin S, Nekovee M and Inglesfield J E 1995 *Phys. Rev.* B **51** 7318
[73] Harris G M, Roberts J E and Trulio J G 1960 *Phys. Rev.* **119** 1832
[74] Graboske H C, Harwood Jr D J and Rogers F J 1969 *Phys. Rev.* **186** 210
[75] Brady B T and Rowell G A 1986 *Nature* **321** 488
[76] Kanorsky S I, Arndt M, Dziewior R, Weis A and Hänsch T W 1994 *Phys. Rev.* B **49** 3645
[77] Kanorsky S I, Arndt M, Dziewior R, Weis A and Hänsch T W 1994 *Phys. Rev.* B **50** 6296
[78] Kanorsky S I and Weis A 1996 *Quantum Optics of Confined Systems* ed M Ducloy and D Bloch (Dordrecht: Kluwer Academic) p 367
[79] Brus L E 1984 *J. Chem. Phys.* **80** 4402
[80] Schmidt H M and Weller H 1986 *Chem. Phys. Lett.* **129** 615
[81] Bastard G 1981 *Phys. Rev.* B **24** 4714
[82] Bryant G W 1984 *Phys. Rev.* B **29** 6632
[83] Brown J W and Spector H N 1986 *J. Appl. Phys.* **59** 1179
[84] Tsonchev S I and Goodfriend P L 1992 *J. Phys. B: At. Mol. Opt. Phys.* **25** 4685
[85] Zhu J-L and Chen X 1994 *Phys. Rev.* B **50** 4497
[86] Kalnins E G, Miller W Jr and Winternitz P 1976 *SIAM J. Appl. Math.* **30** 630
[87] Bluhm R and Kostelecký V A 1993 *Phys. Rev.* A **47** 794
[88] Abramowitz M and Stegun I A 1972 *Handbook of Mathematical Functions* (New York: Dover)
[89] Landau L D and Lifschitz E M 1979 *Lehrbuch der Theoretischen Physik (Quantenmechanik)* vol III (Berlin: Akademie Verlag)
[90] Langer R E 1937 *Phys. Rev.* **51** 669
[91] Kramers H A 1926 *Z. Phys.* **39** 828

[92] Fröman N and Fröman P O 1965 *JWKB Approximation, Contributions to the Theory* (Amsterdam: North-Holland)
[93] Comtet A, Bandrauk A and Campbell D 1985 *Phys. Lett.* **150B** 159
[94] Bestle J, Schleich W P and Wheeler J A 1995 *Appl. Phys.* B **60** 289
[95] Friedrich H and Trost J 1996 *Phys. Rev. Lett.* **76** 4869
[96] Friedrich H and Trost J 1996 *Phys. Rev.* A **54** 1136
[97] Prudnikov A P, Brychkov Yu A and Marichev O I 1992 *Integrals and Series, Vol. 2: Special Functions* (New York: Gordon and Breach)